

# A Cellular Automaton Model of Wildfire Propagation and Extinction

Keith C. Clarke, James A. Brass, and Phillip J. Riggan

## Abstract

*We propose a new model to predict the spatial and temporal behavior of wildfires. Fire spread and intensity were simulated using a cellular automaton model. Monte Carlo techniques were used to provide fire risk probabilities for areas where fuel loadings and topography are known. The model assumes predetermined or measurable environmental variables such as wind direction and magnitude, relative humidity, fuel moisture content, and air temperature. Implementation of the model allows the linking of fire monitoring using remotely sensed data, potentially in real time, to rapid simulations of predicted fire behavior. Calibration of the model is based on thermal infrared remotely sensed imagery of a test burn during 1986 in the San Dimas experimental forest. The model and its various implementations show distinct promise for real-time fire management and fire risk planning.*

## Introduction

Wildfires are those fires which result from natural and man-made causes and which burn land surface cover, mostly vegetation, without effective human control. During 1990, 122,763 wildfires in the United States burned 2.2 million hectares, an area larger than that of Massachusetts. Wildland, rural, and urban areas are threatened. In the urban areas of Santa Barbara in 1990 and Oakland in 1991, wildfires caused significant loss of life and several billions of dollars in damage. Effective means of managing fire risk, therefore, are likely to yield significant benefits to society.

Wildfires have been and still are predominantly a characteristic of the dry western forests and grasslands in the United States. However, the combination of dry summer weather, periodic drought, accumulated dead fuel, and increasing human settlement of fire-prone areas now leave few places immune from fire's damage. Wildfires are usually ignited by lightning, by arson, by accident, or begin when a controlled fire goes out of control. Controlled fire is used extensively both in agriculture, to clear land in swidden (slash and burn) or to burn straw and remove pests from fields after the harvest, and in forestry to manage tree growth and to reduce the risk of wildfire.

From the environmental scientist's point of view, fires

are important in two respects. First, fires have a profound and complex impact upon vegetation; removing species, altering soil chemistry, concentrating nitrogen, removing the surface cover which prevents soil erosion, and even triggering reproduction in some species (Brown and DeByle, 1989). After a fire, precipitation washes soil nutrients into rivers and lakes, transforming aquatic chemistry and ecosystems. When fires burn at high temperatures, or smolder through a thick vegetative cover such as peat, they can completely remove the organic content of the soil, and kill all soil microorganisms, essentially sterilizing the soil.

Secondly, fires are a major source of gases and particulates in the atmosphere, including hydrocarbons, carbon dioxide, carbon monoxide, and ammonia. Recently, scientific interest in the global consequences of increasing the proportion of carbon dioxide in the Earth's atmosphere has become coupled with a greater concern for reducing air pollution. Large wildfires are major sources of particulate contamination in the air, while fires globally, including those used to clear land in the tropics and elsewhere, and those deliberately set as acts of war, are thought to be major sources of the gases which cause the greenhouse effect.

Significant scientific effort has gone into the study of wildfire, especially into thermodynamics, chemistry, and modeling of the parameters associated with fire prediction and control. Less work, however, has gone into modeling or predicting the spatial behavior of wildfire or into the valuable role that remote sensing can play in fire monitoring, though the potential is high (e.g., Chuvieco, 1989). In spite of an extensive body of knowledge on translating fire theory and experimental results into fire management and fire-fighting techniques, few opportunities have been available to fire managers to experiment practically with fire's spatial behavior. Obviously, large scale wildfire experiments are best performed as simulations. Ideally, such wildfire simulations should be performed interactively, so that the consequences of fire control interventions can be seen immediately. Rarely is this possible with real fires, and even then only one course of events can be followed. Real wildfires usually leave behind a fire scar and a human story, but only a very sparse data set on fire behavior. Instrumentation of fires to measure their physical properties is expensive, difficult, and dangerous. Increasingly, however, remote sensing is offering effective monitoring of fires both during and after their incidence.

This paper begins with the basics of fire chemistry and

K. C. Clarke, Department of Geology and Geography, Hunter College, and the Graduate School and University Center, City University of New York, 695 Park Avenue, New York, NY 10021.

J. A. Brass, Ecosystem Science and Technology Branch, NASA Ames Research Center, Moffett Field, CA 94035.

P. J. Riggan, Forest Fire Laboratory, Pacific Southwest Research Station, USDA Forest Service, Riverside, CA 92507.

Photogrammetric Engineering & Remote Sensing, Vol. 60, No. 11, November 1994, pp. 1355-1367.

0099-1112/94/6011-1355\$3.00/0

© 1994 American Society for Photogrammetry and Remote Sensing

physics to introduce the geometric fire behavior model most commonly used in predictive fire modeling. The introduction summarizes a particularly large, energetic, and active fire research literature, and as such is a simplification. A model of fire behavior during the phases of propagation and extinction is then introduced. The model is based on the fractal process of Diffusion Limited Aggregation (DLA) implemented as a cellular automaton, and its approach to fire geometry is examined in contrast with the existing approach. The model was calibrated using remotely sensed data from a test fire conducted in the San Dimas experimental forest in 1986, and simulated data from the model are compared with real data for this fire. Finally, potential applications and extensions of the model and its implementation are considered.

### Fire Chemistry

Fire is a chemical reaction which occurs within a zone defined by the mixing of heat, fuel, and oxygen (Pyne, 1984; Blackshear, 1974). Combustion involves three phases; ignition, propagation, and extinction, which are rarely spatially or temporally distinct. Ignition processes are many and have their own natural and man-made spatial distributions which are beyond the scope of this paper (Fuguay *et al.*, 1979). Ignition, however, is critically affected by the amount of moisture in the air and the fuel when the fire ignition source becomes available. Live fuels can contain 80 to 200 percent of their oven dry weight in water, while dead fuels contain 1 to 30 percent. The range within these percentages is attributable to the species type, the time since it last rained, and the relative humidity of the air. Also, as air becomes hot and dry, fuel is dried and pre-heated to favor ignition. Once ignition occurs, a fire often is extinguished immediately. For fire to continue, fuel at the source must be heated during ignition sufficiently to induce boil-off, the process by which fuel moisture is released as steam. Because the boil-off involves both additional heating and the absorption of latent heat, many fires die at this stage. In addition, lightning is often accompanied by rain.

If ignition is successful, the fire moves on to its period of propagation, characterized by the chemical process of pyrolysis. Pyrolysis is the consumption by fire of fuel, and involves burning both of the fuel itself and of the volatile gases or pyrolysates which are released. The release of the gases can generate winds, which carry the reaction to new fuels. If the fire burns at low temperatures, the principal reaction is the conversion of fuels to tar and char. At higher temperatures, the products are water vapor, volatile gases, carbon dioxide, carbon monoxide, tar, and char. The gases include ammonia and oxygen released from the fuel moisture. The char and ash can contain a high proportion of mineral silicates, which are not combustible and act as an absorber of heat, inhibiting the fire.

During the fire the reaction itself is strongly influenced by the type and distribution of the fuels. Fastest to burn, and with the greatest intensity, are the fine fuels such as leaf litter, pine needles, and grass. Wood burns comparatively slowly, since the critical ratio seems to be the total surface area exposed rather than the type of fuel material. This means that the greatest release of thermal energy takes place in the two or three minutes during which the flaming fire front passes a point, as the light fuels burn. The remaining wood and char, both of which are poor thermal conductors, burn more slowly and far less intensely. Critical factors relating to the fuel are the bulk density, the porosity, and the

packing ratio, which implies that both the amount of fuel and its oxygen content are critical.

The principal constituent of wildfire fuel is cellulose, the major component of wood. At 100°C, the fuel moisture is boiled off and latent heat is absorbed. At 200°C, the principal extractives of the fuel are volatilized. At 250°C the cellulose itself starts to break down, a process which is complete by the time the fire reaches 325°C. Between 300°C and 400°C the woody constituents other than cellulose break down, with yellow and orange flaming appearing between 300°C and 380°C. Above 500°C gasification ends, and the fire appears red or white as char becomes the only fuel. The intensity of the reaction is critical to fire behavior, because it determines the fire front temperature, the flame height, and the width of the flaming zone, important factors to know for fire control. The reaction intensity is defined as the energy released per unit area of ground, in kilojoules per square metre per minute (Wilson, 1980). Reaction intensity, as measured in combustion chamber experiments, is inversely related to the dead fuel moisture content, approaching zero at about 30 percent. However, the relationships are complex, some fuels such as slash showing high intensities at all moisture contents with a rapid drop at 30 percent, others such as timber litter, brush, and short grass showing little variation but low intensities (Rothermel, 1972). Another important factor during pyrolysis is smoke. Smoke can itself be a fuel; loblolly pine smoke, for example, contains 56 organic compounds plus unburned hydrocarbons as particulates (Tangren *et al.*, 1976). Smoke, and its spread, can strongly influence fire behavior and chemistry.

The final stage of fire is extinction. During propagation, fires are self sustaining, but ultimately depend upon spread to find new fuel. As fire moves, the delay time of the new fuels to combustion is critical, and this depends upon the preheating of the fuels, the type and moisture content of the new fuels, and the fire behavior. Once reaction intensities fall, the fire temperature drops below the level at which flaming combustion can take place. At this time, unless other factors such as a wind shift come into play, the fire will burn its remaining char *in situ*, and eventually go out. This final stage, especially in highly organic soils, can take days, weeks, or even months. The burning can remain as a potential source of new ignition when environmental conditions change. When the fire is extinguished, the principal remaining material is ash, with a silicate content dependent upon the mineral composition of the soil and the vegetation. Char remains if large masses of fuel remain partially unburned, e.g., tree stumps.

### Fire Physics

The chemistry of fires is comparatively well understood, and has been the subject of intensive investigation by combustion chamber testing. The physics of fires is far more complex. Of primary concern is the question of fire spread. "Will a fire spread at all, and if so when and how?" are questions upon which millions of dollars and many human lives depend. Virtually all methods of fire control, fire management, and fire fighting are based upon knowledge of fire physics. The pioneering physical model of fire spread was by Rothermel (1972). Rothermel's model is the basis of all United States based fire behavior simulations by computer programs such as FIRECAST (Cohen, 1986) and BURN (Albini, 1976).

Rothermel argued that the propagating heat flux,  $I_p$ , is proportional to the heat required to bring the fire fuel to the point of ignition: i.e.,

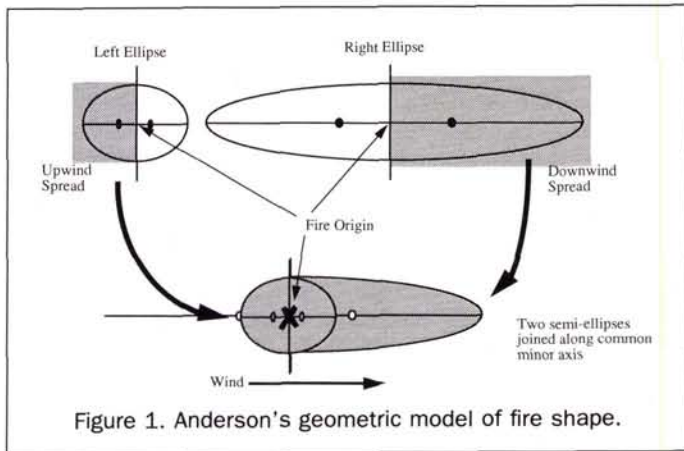


Figure 1. Anderson's geometric model of fire shape.

$$I_p = R(\rho_b \epsilon Q_{ig})$$

which combines the constant of proportionality (the spread rate  $R$  in metres per minute) with the pre-ignition conditions, the product of the oven-dry particle density in  $\text{kg}/\text{m}^3$  ( $\rho_b$ ), a constant ( $\epsilon$ ), and the heat of pre-ignition  $Q_{ig}$  in  $\text{kJ}/\text{kg}$  (Wilson, 1990). The spread rate significantly influences fire geometry and is an important variable for computing fire area, perimeter length, and the fire-fighting variables which go with these values.

The propagating flux is also proportional to the reaction intensity in  $\text{kJ}/\text{min}/\text{m}^2$ , an areal energy release, with a constant of proportionality determined by the fuel bed geometry, such as the packing ratio and the size. This value also represents the amount of energy released, and therefore detected, by remote sensing instruments in the thermal infrared part of the spectrum. Because reaction intensity can also be determined as

$$I_r = -h \left( \frac{dw}{dt} \right)$$

where  $h$  is the fuel particle low heat content in  $\text{kJ}/\text{kg}$  (determined by the type of fuel),  $w$  is the fuel loading in  $\text{kg}/\text{m}^2$  (the density of the fuel), and  $t$  is time in minutes, the equations can be solved for reaction intensity ( $I_r$ ) in terms of the fuel loading, the fuel particle low heat content, the optimum reaction velocity ( $\gamma$ ), and the damping ( $\epsilon$ ) of moisture (sub  $m$ ) and silicate minerals (sub  $s$ ) in the fuel: i.e.,

$$I_r = w_n h \Gamma \eta_M \eta_S$$

These terms can be experimentally determined and, by combination and substitution, allow a solution for the spread rate  $R$ , in  $\text{m}/\text{min}$  (see Wilson, 1990).

This value is related to the directions of two vectors, the slope of the terrain and the wind, each of which has a magnitude and a direction. Only the slope (as a vertical rise/horizontal distance angle) and the "wind coefficient," both scalars, are used. Thus, Roethermel's derivation primarily determines measurable chemical and physical properties of the fire, the fuel, and the combustion, and tells us little about the geography of fire propagation. Very little information is given about the spatial and temporal distribution of the critical fire intensity measure. Unfortunately, few of the critical variables are directly measurable over space using remote

sensing. Those best measured are vegetation type and energy release in the thermal infrared. Slope and aspect are directly measurable using a digital elevation model. Fuel moisture and the soil silicate content, along with several other constants, must be determined either in the laboratory, or by field mapping of soils. Fuel moisture is sufficiently interrelated with topography and insolation that modeling may be possible directly from the DEM.

### Fire Geometry

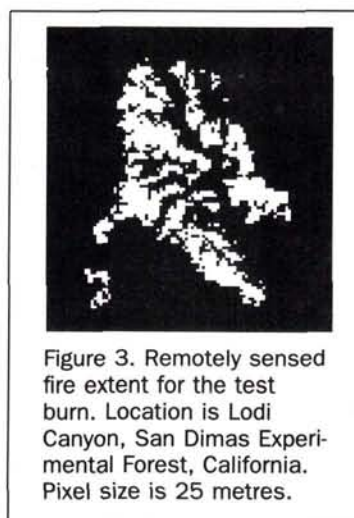
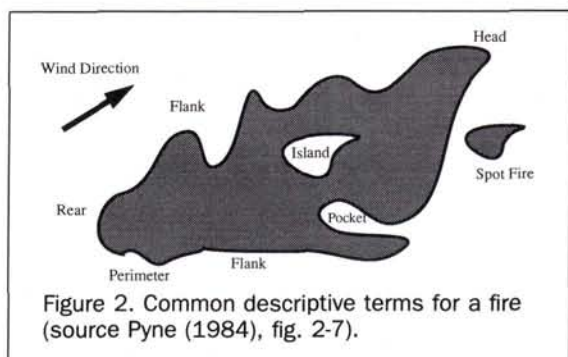
Anderson (1983) developed the currently accepted model of combustion geometry, and his ideas have been incorporated into fire models such as BURN. Anderson built upon some classic results by Fons (1946) of 198 wind tunnel combustion chamber experiments, and a number of well-studied wildfires, such as the Sundance fire and the Air Force Bomb Range fire, both documented by Pyne (1984). Anderson proposed a boundary shape model, in which the periphery of the fire or the fire front forms a figure delineated by two semi-ellipses (Figure 1). By least-squares fits of log regressions of wind speed and amount of forward spread, Anderson (1983, eq. 2-6) produced a set of equations which describe the average fire geometry, and allow the computation of fire area and total perimeter, as well as maximum width, because McArthur (1966) has shown that the length to width ratio of the fire is a function of wind speed.

Anderson used the perimeter and area relationship to examine shape changes in six fires for which data was available. Anderson concluded that, when the wind is stable and the fuels are constant, the fires remain at a constant length/width ratio. Only the Honey, Louisiana fire, however, showed this phenomenon, and then only after ten minutes of rapid spread, and when separate spot fires were considered in isolation. Most of the other fires showed wide variations in shape. Shapes of fires used in the computations show poor approximation to a double semi-ellipse. Deviations are explained away as variations in wind speed, direction, and fuel load differences.

Anderson's shape model has been used extensively to compute critical values related to fires, such as flame height and forward velocity, with critical importance to fire fighting. The model is only a general descriptor of the geometry of a wildfire, and assumes that some of the most critical determinants of fire behavior, wind direction, slope and aspect of topography, fuel load variations, and fire spread rates are either negligible or constant.

Rarely does a wildfire produce a shape which even approximates a double ellipse, and a fire having this shape cannot be expected to maintain the shape for the duration of a wildfire. Pyne (1984), for example, stated "For mathematical analysis, the shape can be considered as a double ellipse. The stronger the wind or slope, the closer the total fire shape will approximate the ellipse. When the fire burns slower, influenced by several factors, more rugged shapes result, for which common terms are necessary." Fires in wind tunnels with uniform fuel beds of consistent packing and invariant fuel density and type exhibit few of the variant characteristics of large scale wildfires, but nevertheless show significant shape variation as evidenced by the variances in the measurements in Fons' data. Three factors alone, the variation in the slopes and aspects of terrain, the non-uniform nature of the fuels and their moisture content, and the varying and turbulent nature of wind, would alter a perfect double ellipse beyond recognition in seconds.

Instead of using geometry, fire managers and firefighters



use the “common” terminology of experience and observation to describe features of a fire (Figure 2). Photographs of fire scars show extreme variation in shape, and even topology. Fire scars are irregular, finger-like, have islands and detached outliers (spots), and show crenulated edges. The outline of the final burned extent for the Lodi Canyon test burn described later in this paper, for example, is shown in Figure 3. One way to model such a shape is to isolate the various factors contributing to the shape and describe their influence independently. In the case of fires, however, the causative variables are both numerous and interrelated. Fuel moisture, for example, depends upon the weather, the type and quantity of the fuel and its packing, and also the amount of shade at the location, itself a function of the topography.

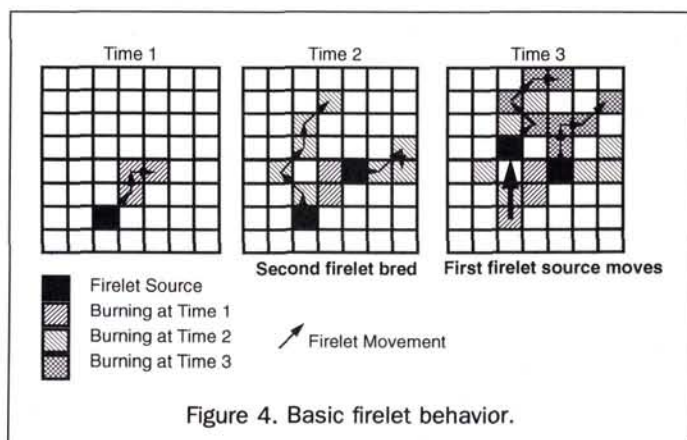
When the interrelationships and strengths of links between causal variables within a system are impossible to determine fully, the system appears chaotic. Chaos theory predicts that a chaotic process, and we suggest that wildfire is a chaotic process, can generate a form whose geometric dimension is fractional or “fractal.” In this case, the wildfire extent, during or after the fire, has a form somewhere between a regular geometric shape such as an ellipse (dimension 2) and a line (dimension 1), filling part of the space between these two extremes. To test this assertion, a fractal measurement algorithm was applied to the boundary of the San Dimas test fire described below and shown as Figure 3. An algorithm was applied to the fire scar’s outline, measuring its extent at several levels of aggregation or equivalent map scales. Least-squares methods were then used to test the relationship between the length of the scar boundary and the grid spacing. The result was a fractal dimension of 1.13, with a coefficient of determination to the log-log regression of boundary edge length versus aggregation level of 0.986 using the method described by DeCola (1991). This is a statistically significant relationship, and we use this result to argue that the fire scars resemble fractals rather than ellipses.

Three reasons suggest themselves for this fractal nature. First, fire physics and chemistry are strongly determined by their fuels, or more precisely by their fuel packing and mix. Fuel packing is determined by a surface-area-to-volume relationship, a relationship whereby fuels burn better as more of their surface area comes into contact with the air. Because fine fuels have a very large surface area, the scaling property, important in defining fractals, is evident. In addition, the fuel mix is important. No real wildfire burns uniform fuel, but a mixture of pine needles, twigs of different sizes, branches, tree trunks, houses, etc. Each type of object, a pine needle for example, has a specific size with a Gaussian distribution about a mean size at any scale, but the whole fuel

mass is a mixture of these objects. As we move between scales in measuring the fuel, the introduction of smaller types of objects into the measurement, from tree branches to twigs for example, increases the total surface area of the fuel in a non-linear fashion. Thus, the phenomenon “fuel” has a combustibility which is dependent upon the scale at which its mass, volume, and surface area are measured. This type of relationship is similar to a fractal property termed self-affinity by Mandelbrot (1985). Thus, critical to a fire is also how many branches per trunk, how many twigs per branch, how many pine needles per twig, etc. This self-affine nature of fire fuels, we argue, results in self-affine aggregate behavior and fractal form during fire propagation.

Similarly, a fractal process leads to fractal forms on the ground, with manifestations at different map scales. At any given map scale, variation is not random, but is influenced by the wind, by the slope and aspect of the topography, by the fuel type and the fire environment, and by chance. Between map scales, however, the scaling property is evident and the result is a different blend of causative factors by map scale.

Second, fires, like fractal forms, are highly sensitive to their initial conditions. A whole new set of fire variables applies to favoring ignition, such as air temperature, preheating of fuels, and the time since the last rain. Even at the time of



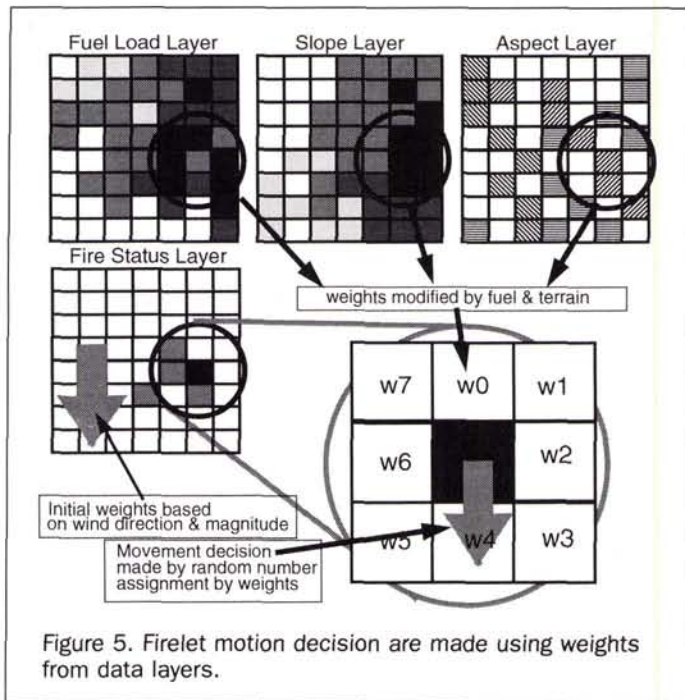


Figure 5. Firelet motion decision are made using weights from data layers.

ignition (itself a somewhat fractal process because lightning and arson are seldom spatially either uniform or random) many fires go out almost immediately, in spite of suitable fire conditions. If the point of ignition is at the top of a ridge versus the bottom, for example, the fire will be of greatly different extent. Should the fire ignite at the bottom of a valley, with no wind, an infinite number of possible fire shapes could result from the same ignition point and the same conditions.

Third, fire spread is self-replicating. Every burning location is capable of igniting those around it, and, if the weather and fire conditions are suitable, fires spread by "spotting," a process by which flaming material is carried downwind to start new fires (Albini, 1979). We propose that self-replication is grounds to suspect self-affinity, both within a single fire and between fires which originate from related sources.

### The Model

The inspiration for the proposed fire model is that fire propagation is a process closely resembling that of diffusion limited aggregation (DLA). DLA is an aggregation process which has been used to explain the growth of snowflakes, mineral crystals, and cities (Batty *et al.*, 1989; Meakin, 1983; Mullins and Sekerka, 1963). DLA is a combination of the well-studied diffusion process with the constraint that growth takes place only onto existing structures. This body of theory has followed from that of fractals, and DLA has been shown to produce objects which are self-affine and scaling, both properties of fractals (Mandelbrot, 1977).

DLA is a process-oriented model, and assumes that an object will grow and change shape due to a large number of essentially random events, each of which is influenced by the events which preceded it. This approach is similar to that used in the cellular automaton game of "life," in which patterns of cells survive or die solely on the basis of the extent to which their neighboring cells are alive. Cellular au-

tomata have been used to simulate long term ecological balances in forests due to fires (Maddox, 1992), but not actual behavior during a fire.

In the context of fires, the cellular automaton can be thought of as a process by which "firelets" are sent out one at a time from a fire source. Ignition consists of the creation of a single firelet. The firelet survives by igniting new fuel and moves in a direction determined by the fire environment, to be defined below. If there is no fuel at the new location, or if the firelet has moved too far from its source, the firelet stops. The next firelet then moves out from the fire center. If this firelet finds a cell which has already been burned, the firelet continues on its journey. Upon finding virgin fuel, the firelet ignites it and stops. When a firelet travels a certain distance determined by the fuel conditions, the firelet goes out (Figure 4). This is a modified DLA process model, because the firelet makes a passage over the existing structure before arriving at the edge rather than the inverse, aggregating to the edge from the exterior.

Implementation of the model is shown in Figure 5. A fire is ignited at a location given by the user, and any number of fires can be started simultaneously or at set times and places. The eight-cell neighbors of any given pixel are then numbered off in octal. These neighbors start with weights assigned on the basis of the wind direction and magnitude. These weights are modified by changing the weights to reflect the topography; up-slope aspects are weighted by the magnitude of the slope. A second modification again changes the weights to reflect the fuel load, taking into account reductions in fuel as it is consumed by the fire. A random number is then drawn to determine direction of movement. The new firelet location is then "burned," and the fire moves on. A "run" will stop when the image edge is reached, when no fuel remains, or when a set distance is reached. Each fire center continues to generate random fire "runs" of a length which reflects the fuel moisture and pre-heating conditions until its firelets find no unburned fuel. When successive runs find no new fuel to burn, this fire center goes out.

In addition, fire spreading centers (unlike in the classical DLA model) are permitted to migrate toward the active fire front, with the direction and magnitude of the movement determined partly at random, and partly to reflect the location of the most active fire front (Figure 4). To further simulate spread, new fire centers are permitted to form at random at the ends of firelets, each of which functions as a new independent fire, making the process recursive and self-similar. The maximum number of simultaneous secondary fires is user determined, and the actual number is a function of total intensity over all fire centers and the preheating of the fuel. Secondary fires can also form at high wind velocities by spotting, i.e., when the total fire intensity crosses a threshold, new spreading centers spontaneously form downwind from the existing fire.

To simulate the combustion process, fires can age in two ways. First, as a run "burns" anew across a pixel, the fire consumes another unit of the fuel at this location. Second, at the end of a spreading phase, burning pixels from all sources are "aged" by allowing additional fuel consumption. This simple mechanism makes the interior of a burning area eventually go out, leaving the active new fire at the front. The mechanism also forces the fire to go out if fire conditions are unfavorable, such as too little wind, not enough fuel, etc. Pixels in the model are assigned a temperature index of between zero and ten, with zero used for unburned and ten for extinguished. The actual temperature profile over time is

TABLE 1. PERCENT PROBABILITY OF FIRELET MOVEMENT FOR NORTH WIND

Octal Wind Magnitude	North	North-east	East	South-east	South	South-west	West	North-west
0	12	12	12	12	12	12	12	12
1	8	10	10	17	18	17	10	10
2	7	9	9	18	21	18	9	9
3	6	8	8	18	26	18	9	8
4	5	7	7	19	29	19	7	7
5	4	6	6	20	32	20	6	6
6	3	5	6	22	31	22	6	5
7	2	4	5	24	32	24	5	4

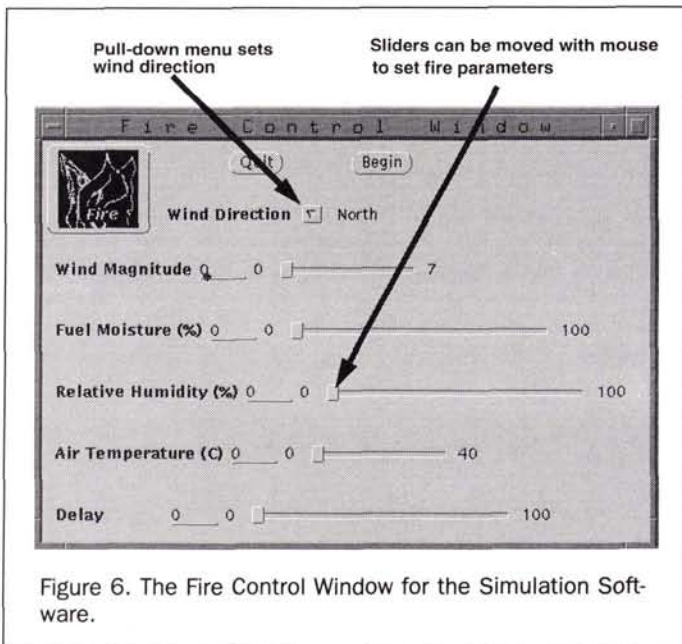


Figure 6. The Fire Control Window for the Simulation Software.

probably a function of the condition of neighboring pixels and the fuel load. Peak fire temperatures are usually in the burning zone just behind the front.

The computer version of the model uses a pseudo-random number generator seeded by the system process identification number, and therefore produces similar, but never identical, fires in successive runs. Input variables for the fire consist of a fuel map, a terrain map, a wind table, and values for the wind magnitude and direction, the air temperature and relative humidity, and the fuel moisture content. Both an interactive and a Monte Carlo version of the model were produced. The latter version runs without graphics but performs many iterations of the fires and averages the results.

Many other factors are controlled in the model, their values having been set by calibration with the Lodi Canyon data. These include rates of spread, maximum permitted number of new fires and the rate of self replication, weighting factors for terrain slope, and extinction conditions. Each of these factors is partially linked, however, to one or more of the input variables, and is therefore partly under user control. The model has no smoke component, a severe limitation, because smoke affects preheating, the flaming front, shadows, etc. Wind is also assumed uniform and without vertical structure or turbulent interaction with either the ter-

rain or the fire. Finally, the model assumes that ignition is determined by the user or at random, and has no component to simulate lightning or any other fire ignition process.

Fire factors not yet included in the model are specific calorimetric values for fuels, details of fuel types, fuel packing ratios, and wind variability. Currently, no fires are allowed to be subjected to dynamic variations in conditions, i.e., once a run is started, conditions must remain fixed until the end. Minor changes to the user interface, however, will allow both real-time and programmed changes in fire environment.

### Implementing the Model

The fire model proposed, based on the modified DLA process, was implemented in the C programming language under the UNIX operating system and using a graphics workstation. Test data for the model was for the Lodi Canyon area as described below, and consisted of a 30-metre Digital Elevation Model from the U. S. Geological Survey (USGS), which was resampled at 25 metres for the test data set. The study area covered two branches of Lodi Canyon and some surrounding hillsides for an area 5.8 km wide by 5.75 km long sampled by 53,360 pixels at a 25-metre spacing. In the absence of any real fuel loadings for the area, the red channel reflectances (1 byte) from the Daedalus Thematic Mapper Simulator were used as an estimate of fuel load, a factor which will be corrected using field and multispectrally classified remote-sensing data in future tests. The wind table probabilities (Table 1) were derived from the ellipses shown in Figure 1. When the wind has no magnitude, the fire has a 12 percent chance of moving in any direction (rounded to 12.5 percent). As the wind increases in magnitude, from 0 to 7, the directionality becomes more pronounced.

The wind probabilities were loaded into an array inside the program, and were rotated to apply to any given wind direction. The probabilities were assigned, and then the level increased in the direction of the maximum uphill slope (the opposite of the aspect and the two adjacent directions), in amounts proportional to the slopes there. Thus, steep slopes are weighted higher. During the firelet propagation, a random number between zero and seven is drawn to choose the direction, and then a random number between zero and 100 is drawn. If the number is less than the weighted probability level, then the firelet moves in this direction.

The user interface for the program was chosen to give the maximum level of user control and information about the fire. The graphical user interface was written using X-windows and the X-View GUI toolbox. The display consists of three windows. The fire control window (Figure 6) contains sliders for the critical variables, which are moved using the mouse. Wind directions are chosen from a selection list. Once the user clicks the BEGIN button, the fire starts to burn. The program can set any given number of fires at random, or from a pre-set list stored in a file. The fires can be started at any time, so that a user can set backfires to try and control the main fire.

The fire, once burning, is displayed in color over a grey-scale map of the slope aspects for the fire area (Figure 7). The display is updated once at the end of each time period, defined as one run of firelets for all fires which are burning. The program keeps a list of burning fires, and ages them at the end of time periods. A third window is a status display, showing updated graphs of heat, fire intensity, number of fire centers, and percentage of area burned, plus a histogram of the temperature structure of the fire. In addition, the display shows a clock, increasing in ten-minute increments while the

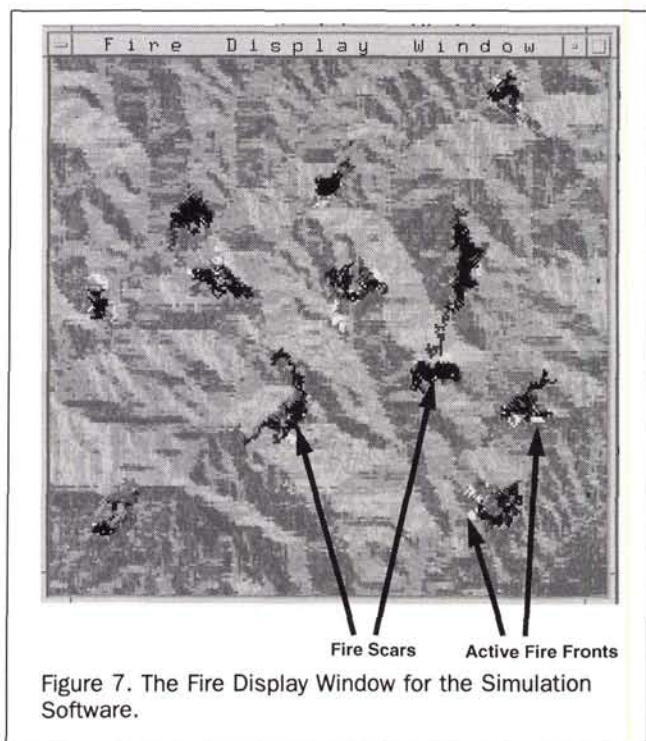


Figure 7. The Fire Display Window for the Simulation Software.

fire burns. The interactive nature of the software can be enhanced by slowing down the speed at which the clock and therefore the program runs, using the slider for delay. Once the fire goes out, a binary image of the fire scar, plus the statistics shown in the status window, are automatically saved on disk, for analysis with display software or with spreadsheet programs.

### Calibration: The Lodi Canyon Fire of 1986

The model was calibrated using data from the Lodi Canyon controlled burn at the San Dimas Experimental Forest, near Glendora, California in December of 1986. This was a typical range fire, of a type which is duplicated hundreds of times annually in the western and southwestern United States. The fire was deliberately started by helicopter napalm torch at 1850 GMT on 12 December 1986, and burned for about five hours. The 425 hectare fire consumed an average of 77.5 Megagrams of fuel per hectare of range scrubland, a total of  $3.3 \times 10^7$  kilograms. The fire smoke plume, 3.5 km high, was responsible for about one percent of the total particulate content of the air mass over all of southern California, and released large amounts of  $\text{NH}_3$ , NO, CO, and  $\text{CO}_2$  both during and after the fire (Cofer *et al.*, 1988a; 1988b).

During the fire, NASA Ames' ER-2 Aircraft conducted 26 overflights at ten minute intervals at an elevation of over 9000 metres. The ER-2 was equipped with a Daedalus Thematic Mapper Simulator (TMS), a scanner with ten electromagnetic bands. The TMS band 10, the thermal infrared band at about 10 to 12 micrometres, has been used extensively to show fire through smoke, though it tends to saturate in the fire itself, missing the full temperature structure. Plate 1 shows a visible light (4,3,2) image from the fire at 2000 GMT, contrasted with a false-colored single-band image from the infrared (band 10). The 26 infrared images covering Lodi Canyon, at a 25-metre ground resolution, were isolated and

moved onto a workstation for analysis. The dataset size was 230 rows by 232 columns.

Digital Elevation Model (DEM) data for the Glendora quadrangle was provided by the USGS. The DEM was read from tape, resampled from 30 to 25 metres, and used to compute slope and aspect for the pixels in the TMS imagery. The TMS imagery was then subjected to further analysis in order to better understand the properties of fire spread. The spread of the fire was visible in these images, and showed a distinct pattern. Clearly of great importance were the wind direction, the slope and aspect of the topography, and the fuel loadings. The fire showed a pattern of three distinct stages, which itself was repeated three times during the Lodi Canyon fire. The fire phases were an ignition phase, in which the fire is linear due to the helicopter flight, a rapid propagation phase, in which the fire gains both areal extent and begins to show a branching structure, and thirdly an extinction phase, in which the original fire source goes out, and the branches become multiple new fire fronts, with some going out and some spreading to seed the next cycle.

Details of this structure were established by using a computer program which computed the shape transform of the fire areas burning at a threshold temperature, a method known as a medial axis transform. This method was thought to be particularly suitable to fire data, because the technique is often called the "prairie fire" method. The technique reduces a shape to a "skeleton" which is a complete descriptor of the geometry and topology of the object (Rosenfeld and Kak, 1978). Spatial complexity is given by the depth and number of branches in this skeleton. Collapsing the skeleton onto its most "connected" point allowed after-the-fact deduction of the fire start locations, i.e., the places where the helicopter dropped the napalm. Statistical analysis of the fire images, the medial axes, and other research greatly assisted in making the simulations behave more like a real fire; for example, the ability of the fire to replicate itself was added to simulate events during the fire.

Calibration of the model was in two steps. First, a set of environmental measures was produced to match the Lodi Canyon fire. Holding these constant, the model was then calibrated by subtle changes in the behavioral criteria of the cellular automaton based on the spatial pattern of the burning fire, its temperature structure, and its temporal pattern. Statistics for the calibration are shown in Figure 8. In general, the model seems to overestimate burned areas at high temperatures and underestimate at low temperatures. This may be due to the saturation in the thermal IR of the TMS sensor, which would tend to underestimate the high temperatures in the observed data. A slight lag in the time steps is due to the fact that the model takes one to two steps to respond to the environmental and geographic variables. A cumulative description of the areas is shown as Figure 9. From this graph, it is evident that the model underestimates the actual area burned, mostly by underestimating the flare-up/die-back nature of the actual fire. These figures are averages over ten fires, and as such may smooth out variations.

The cumulative perimeter of the fire was estimated by counting edge pixels and considering each to have a length of 25m. Also computed was the perimeter length of a geometric single ellipse having a length to width ratio of 7.35, the average of the high and low values quoted by Anderson (1983, p. 6). The ellipse is close to the current geometric model of fire extent, and replaces a fragmented shape with only a single ellipse, which explains the underestimate of the actual fire perimeter. In spite of this, the ellipse is a

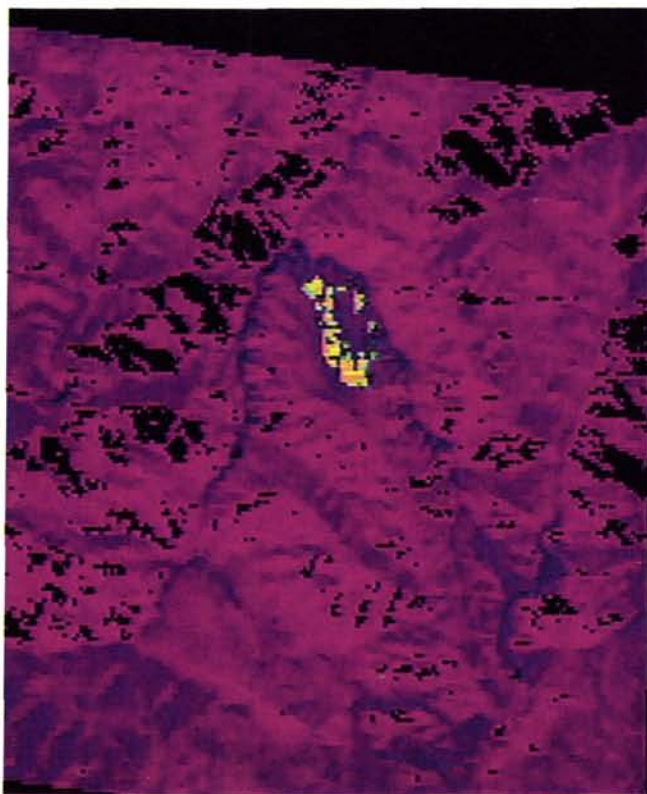


Plate 1. Visible light (4,3,2) image of the Lodi Canyon fire at 2000 GMT, 12 December 1986, contrasted with a false-colored single-band image from the infrared (band 10). Images are from the Daedalus Thematic Mapper Simulator, with a ground resolution of 25 metres.

good statistical model of fire perimeter for the first hour of the fire, as suggested by Anderson, although a weak spatial model. After this time, the cellular automaton simulation provides the better estimate, though the estimates diverge after about 3.5 hours. The fractal nature of the model continues to produce "edginess," a variance which may actually be masked in the observed data by the remote sensing process.

With the calibration over the duration of the fire for aggregate statistics complete, calibration beyond the fire environment parameters of the Lodi test burn could then take place. First, results from 100 simulated fires under the same environmental conditions were compared to the actual burn as shown in the TMS imagery. Burning pixels were extracted from the 26 images and the burning pixels cumulated. The real Lodi fire burned a total of 1636 pixels. Total numbers of pixels were counted for the union of the actual and the predicted fires. Complete agreement would give a 100 percent overlap between the predicted and the really burned pixels. Some untouched pixels were predicted to have burned, and vice versa. The 100 trials allowed calculation of risks. Thus, a pixel which escaped the simulated fire 73 times but was burned 27 times would be considered at a 27 percent risk. With such a relatively low risk, this pixel would be considered unlikely to have been burned in the real fire.

Table 2 shows the results of comparing the predictions to the reality of the Lodi burn. The pixels from the 100 trials were classified into two groups, those pixels with a greater than even chance of burning, and an aggregate number of pixels with a non-zero probability. For pixels predicted by the Monte Carlo version of the model to have any risk of fire, the model scored only 37.5 percent correct for the real fire. Predictions of total safety were incorrect for 18.8 percent of the pixels. Using a 50 percent chance (greater than even odds) as "likely to burn," the model predicted 77.9 percent of the actually burned pixels correctly. It should be noted that the actual and predicted fires are independent, because although the prediction was derived from a model calibrated from the real fire data, the entire simulation can be executed without knowledge (at least after the fact) of the real fire.

The model was then altered so that environmental conditions, the fuel moisture, temperature, relative humidity, and wind direction and magnitude, were assigned at random within their anticipated ranges. Fuel moisture was constrained to the 0 to 30 percent range, because the large numbers of immediate extinctions at the fire sources which would have resulted would bias the results. The real fire can be seen as a single instance from a set of random environmental parameters, and in this case the model does a better predictive job. Overall, non-zero probabilities assigned by the



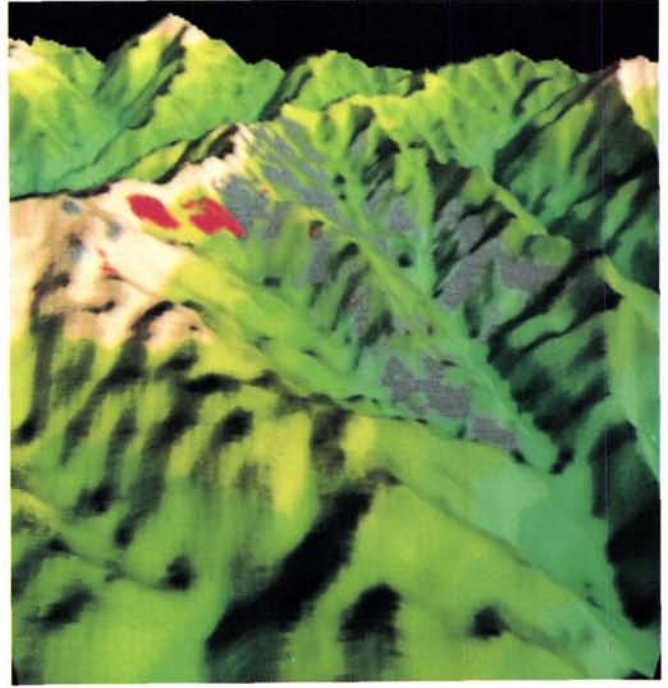
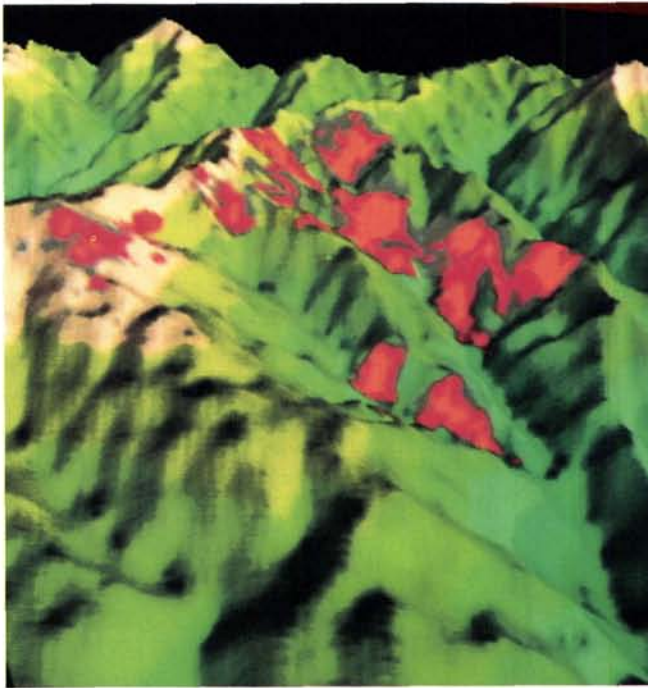


Plate 2. Still frames from the Fire Model Visualizaiton video tape. Perspective view of model runs using the Lodi Canyon data from the south.

model were correct for only 31.4 percent of the burned pixels. However, using the greater than even odds criterion, the simulation produced a fire map which was 82.5 percent correct on a pixel basis, and for the pixels predicted as more than 80 percent likely to burn, was correct for 29 out of 33 pixels. Further calibration testing is required over a broader range of fire conditions to draw broad conclusions, but at least for the Lodi calibration data set, the model seems to perform well as a predictive tool.

### Applications of the Fire Simulator

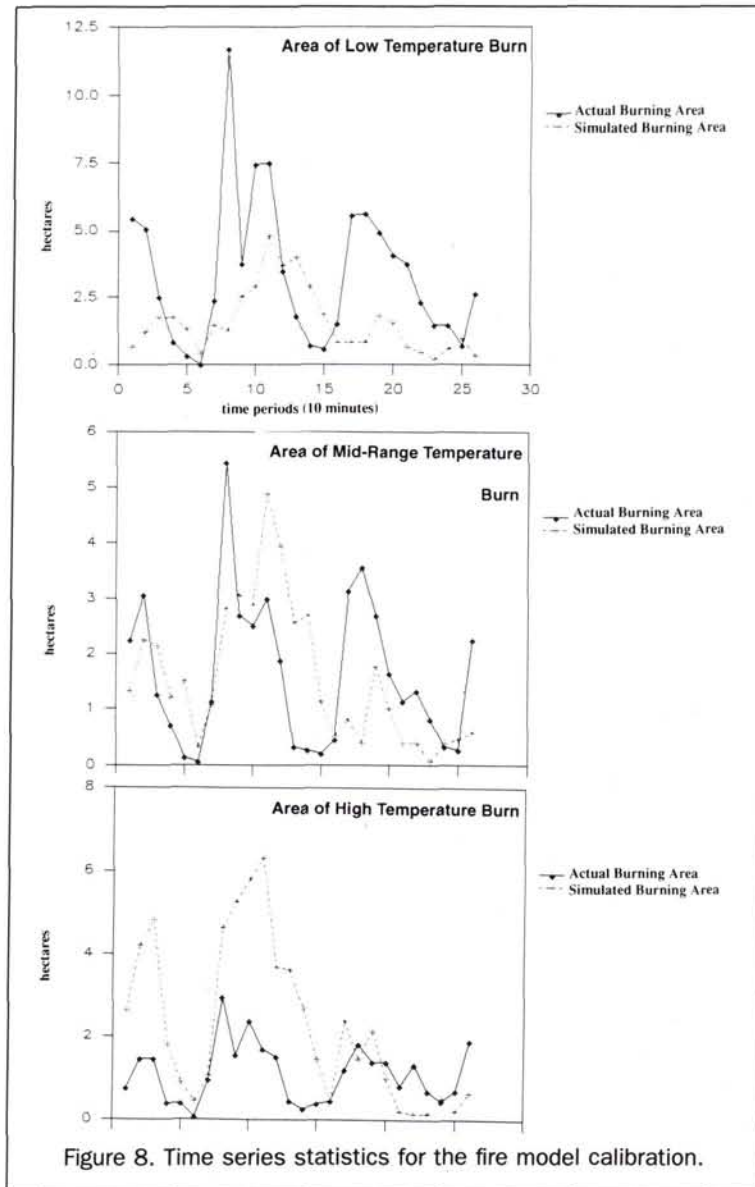
Three sets of applications have been investigated. First, the interactive graphics software has been used on an experimental basis, chiefly to improve the way interaction takes place. A next step would be to investigate using the software as part of a fire management training program, using it first with fire experts until they are satisfied with the model's calibration. Improvements to the software to add a preprocessor which sets up ignition points in advance over a time span would be more consistent with the typical fire plan, which involves multiple ignitions at several places and at different times. To assist in this process, both the software itself and a videotape have been produced to demonstrate the software's capabilities. Two frames from the videotape are shown as Plate 2. Additional test data sets, as well as synthetic test surfaces like cones and flat planes, have been and continue to be developed.

Second, the Monte Carlo version of the software has been used to produce maps showing percentage likelihood of any area being burned, given different sets of circumstances.

Figure 10 shows the result of having 100 fires ignited in the same places and times as the 12 December 1986 burn in Lodi Canyon with a south wind at force 1, and with 15 percent fuel moisture, 25°C air temperature, and 50 percent relative humidity. As large numbers of fires burn, the aggregate fire tends toward a double semi-elliptical shape facing uphill and downwind. However, there is clear evidence that large deviations from this shape are to be expected. Notable also is that the fire shows high probability of branching along topographically determined channels, implying that, in the aggregate, fires are primarily topographically determined.

Even in the absence of fuel data, for example, assuming uniform fuel, and without real weather data, a simulated fire risk map can be generated. When the map is produced from real vegetation data, real topography, and known data about the weather and fuels, we deduce from the initial calibration statistics that accurate and useful maps can be produced. Far more intriguing as an application, however, is to use the model to predict the behavior of fires already in progress. The NASA-Ames ER-2 and C-130 aircraft have successfully demonstrated the ability to download infrared scanner data to a workstation either in the aircraft, or on the ground in real-time. With a fourth "window," the interactive software would allow the real-time update of fire environmental conditions, and the experimentation with simulated fire outcomes. The ability to model behavior in this way would allow a fire manager to try out several different fire-fighting strategies, and select the one with the most desirable outcome for implementation.

Furthermore, fire probability maps for different average



weather conditions with known variance can be generated using Monte Carlo simulation, and the results used to produce maps for those responsible for public safety. The general public has been able to make decisions based upon probabilities associated with weather for some time, and should be given access to fire hazards in the same way, both on a fire emergency and on a planning basis. Should prospective builders, land developers, and public officials also have access to meaningful fire hazard maps, many of the risks to life and property from wildfires may be avoidable, or at least manageable, in the first place. Perhaps the model could also guide the redesign or design of new fire protection for existing structures in high fire risk areas.

### Conclusion

A new fire behavior model, based upon a modification of the fractal growth process of diffusion-limited aggregation, has

been proposed, and is the basis for two computer implementations of the model, one interactive and one probabilistic. The model was calibrated and tested using data from the Lodi Canyon fire in the San Dimas experimental forest in December of 1986.

The Lodi Canyon data set is useful to help users of the model understand the model parameters and use of the software. The images are 230 rows by 232 columns, and correspond to a ground spacing of 25 metres. The size of this data set is sufficiently small as not to challenge the computational limits of workstations. Eventual uses of the model will include the coverage of one 7 $\frac{1}{2}$ -minute quadrangle at 30 metres, corresponding to about 450 rows by 350 columns, and using rectified satellite image data sets as determinants of fuel loadings. Spectral classification of these images and ground samples of measured vegetation type, biomass quantity, and fuel packing could greatly assist in the absolute calibration of the model, because these thermal constants are

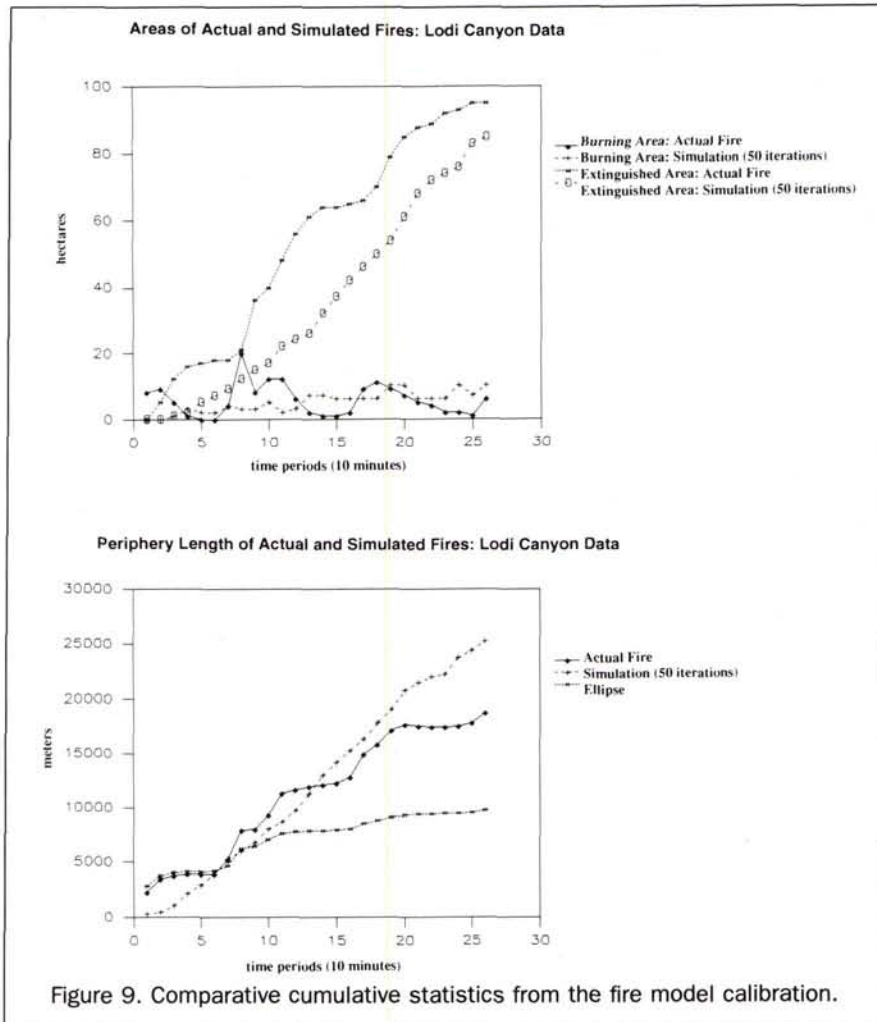


Figure 9. Comparative cumulative statistics from the fire model calibration.

known for many species, and can simply be looked up. This line of research is planned as a next step. Similarly, more and better remotely sensed fire and ground truth data would help in refining the model. Extensions to other fire test data sets will also be pursued as further research. The model's principal strength is its ability to link newly available real-time thermal remote sensing data from infrared detectors on aircraft with fire behavior models in a timely manner. The real-time nature of the data capture, when coupled with a rapid, faster-than-real-time predictive capability may offer significant opportunities for saving life and property.

From a fire science standpoint, the model provides a basis for predicting the critical physical and chemical releases during a wildfire, perhaps allowing integration of the model with ecosystem and atmospheric models. Fire science has developed an extensive body of theoretical and applied chemical and physical research without the benefits of real-time mapping and the power of geographic information management. The model offers the opportunity to test spatial behavior and intervention hypotheses in addition to the modeling of physical fire parameters.

Finally, wildfire may be one of only several natural

processes which diffuse across landscapes with fractal behavior, creating self-affine forms. Species dispersal, move-

TABLE 2. COMPARISON BETWEEN ACTUAL LODI CANYON FIRE AND 100 MODEL ITERATIONS USING IDENTICAL AND RANDOM FIRE ENVIRONMENTAL CONDITIONS.

Fire Risk 100 Burns	Number of Pixels Predicted to burn		Percent Correct
	Number of Pixels Predicted to burn which DID burn	Number of Pixels Predicted to burn which did NOT burn	
SAME ENVIRONMENT Greater than even odds	262	74	77.9
SAME ENVIRONMENT Greater than no chance	1329	2210	37.5
RANDOM ENVIRONMENT Greater than even odds	175	37	82.5
RANDOM ENVIRONMENT Greater than no chance	1389	3028	31.4



Figure 10. Probability map for the Lodi Canyon burn derived from 100 model iterations using the same fire environment. Black is 0 percent, dark gray is 1 to 25 percent, mid gray is 26 to 50 percent, and white is greater than 50 percent.

ment of atmospheric contaminants, plant diseases, and ground pollution may be just a few of the environmental processes which could be modeled using a similar approach. At the very least, fractals and cellular automata allow a new and more natural way of perceiving the spatial diffusion process in the single environmental context of wildfire.

### Acknowledgment

This work was initially conducted at the National Aeronautics and Space Administration's Ames Research Center while the primary author held two consecutive Summer Fellowships sponsored by NASA, the Department of Aeronautics and Astronautics at Stanford University, and the American Society for Engineering Education. Thanks go to David L. Peterson of NASA Ames and to the staff of the ASEE Fellowship Program. Work was completed while the principal author held a visiting scholar position (IPA) in the Office of Research, National Mapping Division, United States Geological Survey. Thanks also to Lee DeCola of the U. S. Geological Survey who performed the computation of the fractal dimension of the Lodi Canyon fire scar, Vincent Ambrosia of TGS at NASA Ames, who provided the Lodi Canyon TMS imagery and to Len Gaydos of the U. S. Geological Survey who provided the DEM for Glendora, California. Three anonymous peer reviewers greatly improved the final manuscript.

### References

- Albini, F. A., 1976. *Computer-Based Models of Wildland Fire Behavior: A Users Manual*, USDA Forest Service unnumbered publication, Intermontane Forest and Range Experiment Station, Ogden, Utah.
- , 1979. *Spot Fire Distance from Isolated Sources: Extensions of a Predictive Model*, Forest Service Research Note FSRN/INT-309.
- Anderson, H. E., 1983. *Predicting Wind-Driven Wild Land Fire Size and Shape*, USDA Forest Service, Intermountain Forest and Range Experiment Station, Research Paper INT-305, Ogden, Utah.
- Batty, M., A. S. Fotheringham, and P. A. Longley, 1989. Urban growth and form: Scaling, fractal geometry, and diffusion-limited aggregation, *Environment and Planning A*, 21:1447-1472.
- Brown, J. K., and N. V. DeByle, 1989. *Effects of prescribed fire on biomass and plant succession in Western Aspen*, Forest Service Research paper, FSRP/INT-412.
- Blackshear, P. L. (Editor), 1974. *Heat Transfer in Fires: thermophysics, social aspects, economic impact*, J. Wiley, New York.
- Chuvieco, E., 1989. Multitemporal analysis of TM (Thematic Mapper) Images: Application to forest fire mapping and inventory in a mediterranean environment, *ESA, European Coordinated Effort for Monitoring the Earth's Environment. A Pilot Project Campaign on Landsat Thematic Mapper Applications (1985-1987)*, pp. 271-285.
- Cofer, W. R., J. S. Levine, P. J. Riggan, D. I. Sebacher, E. Winstead, J. A. Brass, and V. G. Ambrosia, 1988a. Trace gas emissions from a mid-latitude prescribed chaparral fire, *Journal of Geophysical Research*, 93(D2):1653-1658.
- , 1988b. Particulate emissions from a mid-latitude prescribed chaparral fire, *Journal of Geophysical Research*, 93(D5):5207-5212.
- Cohen, J. D., 1986. *Estimating Fire Behavior With FIRECAST: User's Manual*, United States Department of Agriculture, Forest Service, Pacific Southwest Forest and Range Experiment Station, General Technical Report PSW-90.
- DeCola, L., 1991. *Multifractals in Image Processing and Process Imaging*, United States Department of the Interior, U. S. Geological Survey, Open-File Report 91-301, Reston, Virginia.
- Fons, W. T., 1946. Analysis of fire spread in light forest fuels, *Journal of Agricultural Research*, 73(3):93-121.
- Fuguay, D. M., R. G. Baughman, and D. J. Latham, 1979. *A model for predicting lightning fire ignition in wildland fuels*, Forest Service Research paper FSRP/INT-217.
- Maddox, J., 1992. Forest fires, sandpiles and the like, *Nature*, 359: 359.
- Mandelbrot, B. B., 1977. *Fractals: Form, Chance and Dimension*. Freeman.
- , 1985. Self-affine fractals and fractal dimension, *Physica Scripta*, 32:257-260.
- Meakin, P., 1983. Diffusion-controlled cluster formation in two, three, and four dimensions, *Physical Review A*, 27:604-607.
- McArthur, A. G., 1966. *Weather and Grassland Fire Behavior*, Leaflet No. 100, P.D.C. 431.1-431.6. Canberra, Australia: Forest Research Institute, 21 p.
- Mullins, W., and R. Sekerka, 1963. Morphological stability of a particle growing by diffusion or heat flow, *Journal of Applied Physics*, 34:323-329.
- Pyne, S. J., 1984. *Introduction to Wildland Fire: Fire Management in the United States*, J. Wiley, New York.
- Rosenfeld, A., and A. C. Kak, 1978. *Digital Picture Processing*, New York, Academic Press.
- Rothermel, R. C., 1972. *A Mathematical Model for Predicting Fire Spread in Wild Land Fuels*, USDA Forest Service, Intermountain Forest and Range Experiment Station, Research Paper, INT-115, Ogden, Utah.
- Tangren, C. D., et al., 1976. Contents and effects of forest fire smoke, *Southern Forest Fire Laboratory Personnel, Southern Forestry Smoke Management Guidebook*, U.S. Forest Service, General Technical Report SE-10, pp. 9-22.
- Wilson, R. A., 1980. *Reformulation of Forest Fire Spread Equations in SI Units*, USDA Forest Service, Intermountain Forest and Range Experiment Station, Research Note, INT-292, Ogden, Utah.
- , 1990. *Reexamination of Rothermel's Fire Spread Equations in No-Wind and No-Slope Conditions*, USDA Forest Service, Intermountain Forest and Range Experiment Station, Research Paper, INT-434, Ogden, Utah.

(Received 9 December 1992; accepted 2 February 1993; revised 25 March 1993)



### Keith C. Clarke

Professor at Hunter College and at the City University of New York Graduate School and University Center, holds the M.A. and Ph. D. degrees from the University of Michigan, specializing in Analytical Cartography. He is North American Editor of the *International Journal of Geographical*

Information Systems, author of *Analytical and Computer Cartography*, Prentice Hall (1990), and has about 30 publications in the fields of cartography, remote sensing, and

GIS. Dr. Clarke recently served as Science Advisor to the Office of Research, National Mapping Division of the U.S. Geological Survey.

# International Symposium on Spatial Accuracy of Natural Resource Data Bases

*Unlocking the Puzzle*

16-20 May 1994, Williamsburg, Virginia

Russell G. Congalton, Editor

1994. 280 pp. \$65 (softcover); ASPRS Members \$40. Stock # 4536.

The International Symposium on Spatial Accuracy of Natural Resource Data Bases was organized to bring together a group of individuals with common interest in the spatial accuracy of natural resource data bases so that the latest information could be exchanged, and to develop communication pathways that will hopefully long outlive the meeting.

The workshop was sponsored by the International Union of Forestry Research Organizations Forest Inventory and Monitoring Subject Group (S4.02) and the American Society for Photogrammetry and Remote Sensing (ASPRS). The workshop was also endorsed by the Society of American Foresters, GIS Working Group.

This volume of proceedings is a collection of 32 papers that were presented at that meeting, and they dealing with almost every aspect of spatial accuracy in the natural resources area.

## Topics Include:

Session 1 -	Importance of Accuracy I	Session 8 -	Dealing With Accuracy I
Session 2 -	Importance of Accuracy II	Session 9 -	Dealing With Accuracy II
Session 3 -	Accuracy of Basic Data I	Session 10 -	Remote Sensing II
Session 4 -	Accuracy of Basic Data II	Session 11 -	Dealing With Accuracy II
Session 5 -	Example Applications I	Session 12 -	Example Applications III
Session 6 -	Remote Sensing I	Session 13 -	Example Applications IV
Session 7 -	Terrain DEM's		Posters

For details on ordering, see the ASPRS store in this journal.